

---

# HANDSONVLM: VISION-LANGUAGE MODELS FOR HAND-OBJECT INTERACTION PREDICTION

**Anonymous authors**

Paper under double-blind review

## ABSTRACT

How can we predict future interaction trajectories of human hands in a scene given high-level colloquial task specifications in the form of natural language? In this paper, we extend the classic hand trajectory prediction task to two tasks involving explicit or implicit language queries. Our proposed tasks require extensive understanding of human daily activities and reasoning abilities about what is happening next given cues from the current scene. We also develop new benchmarks to evaluate the proposed two tasks, Vanilla Hand Prediction (VHP) and Reasoning-Based Hand Prediction (RBHP). We enable solving these tasks by integrating high-level world knowledge and reasoning capabilities of Vision-Language Models (VLMs) with the auto-regressive nature of low-level ego-centric hand trajectories. Our model, *HandsOnVLM* is a novel VLM that can generate textual responses and produce future hand trajectories through natural-language conversations. Our experiments show that *HandsOnVLM* outperforms existing task-specific methods and other VLM baselines on proposed tasks, and demonstrates its ability to effectively utilize world knowledge for reasoning about low-level human hand trajectories based on the provided context.

## 1 INTRODUCTION

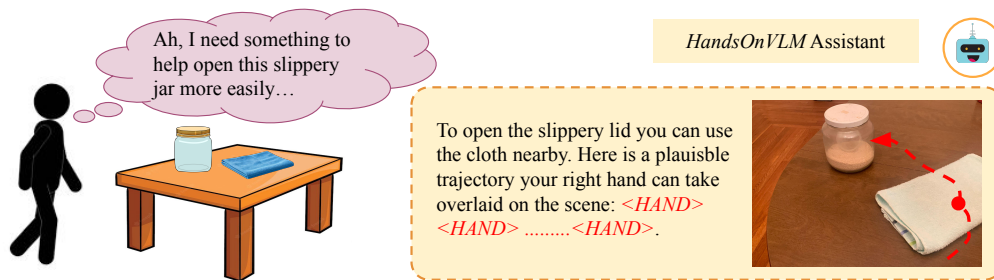


Figure 1: *HandsOnVLM* forecasts low-level actions in the form of hand trajectories in the user’s egocentric view of a scene when queried with a question via natural language.

Humans interact with the everyday world and express themselves with informal and oftentimes vague language descriptions. Consider the example in Fig. 1 - when we try to open the jar, we might think, “Ah, I need something to help open this slippery jar more easily.” We are uncertain about *what* we want exactly as well as about *how* to come up with a solution. To build a computational system for addressing this need, we would require a good understanding of what tools we have lying around (visual scene understanding), general apriori experience of opening jars (reasoning ability and world knowledge priors), and the ability to actually execute the necessary actions for opening the jar (low-level trajectory). In this paper, we develop two language-conditioned tasks for tackling this problem, propose benchmarks for evaluating progress on these tasks, and build a vision-language model (VLM) for predicting low-level hand trajectories in a user’s egocentric view of a scene given colloquial language queries.

Towards a similar goal, some prior works have focused on identifying human intentions based on egocentric human videos of daily activities (high-level intentions of the form “cutting pepper”,

“washing plates”) (Krishna et al., 2017; Grauman et al., 2022; Kahatapitiya et al., 2024), while others have focused on predicting low-level actions such as hand trajectories given human action clips (Liu et al., 2022; Zhang et al., 2024b) without conditioning the predictions on detailed language descriptions of the task to be performed. Both these scenarios are a bit restrictive since for most everyday tasks (e.g. in Fig. 1) we need a combination of high-level reasoning of what to do in a scene and low-level understanding of how to interact with the relevant objects in the scene.

By drawing on the recent successes of VLMs for high-level reasoning (Liu et al., 2024; Lai et al., 2024; Cheng et al., 2024) and advancements in hand reconstructions from generic web videos (Shan et al., 2020b; Rong et al., 2020; Pavlakos et al., 2024), we develop a system for future hand trajectory prediction given conversation-style language instructions. Current best multimodal VLMs are good at predicting semantic actions in the form of *what* is happening at a certain point in a video (Maaz et al. (2023); Huang et al. (2024)), interpreting what objects are in a scene (Achiam et al., 2023) and natively support free-form language conversations for conditioning. However, they are not good at directly predicting *low-level* actions (in the future) of the form of hand-object trajectories. At the same time, recovering low-level interactions in videos, like hand meshes (Pavlakos et al., 2024), object meshes (Fan et al., 2024), and regions of interactions (Shan et al., 2020b; Goyal et al., 2022) has independently become very reliable in recent years. Our key insight is to fine-tune a pre-trained VLM with auto-regressive trajectory predictions of human hand positions, given a few seconds of video and a language description of the task.

Our approach *HandsOnVLM* casts hand trajectory prediction as an auto-regressive next token prediction conditioned on fused video and language tokens. We develop *HandsOnVLM* as an interactive chat assistant that we can query with informal instructions of the form, “Where should my hand move if I want to open the refrigerator?” and a video (or an image) of a scene, and obtain outputs of the form, “To open the refrigerator, the predicted hand trajectory is  $\langle HAND \rangle$ , ....  $\langle HAND \rangle$  ” The *HandsOnVLM* model first converts the RGB video context to visual tokens and fuses them with the language tokens through slow-fast pooling (Huang et al., 2024) for capturing temporal information from the context video at a fine resolution. We extend the vocabulary to add a new  $\langle HAND \rangle$  token, and output a sequence of text and hand tokens. We finally have a trajectory decoder to convert the hand tokens to a sequence of 2D positions of the left and right hands over the prediction horizon.

In summary, our paper has the following contributions:

- We develop *HandsOnVLM*, a novel VLM that can generate textual responses and produce future hand trajectories through conversations by expanding the original vocabulary with hand tokens and having iterative position encodings for auto-regressive predictions during inference.
- We extend existing traditional hand prediction tasks to two new tasks, Vanilla Hand Prediction (VHP) and Reasoning-based Hand Prediction (RBHP), to predict hand trajectories from ego-centric human videos conditioned on language queries of different forms.
- We develop benchmarks for evaluating progress on the VHP and RBHP tasks which we will open-source to the community, in addition to our trained models on the benchmarks.

Our results on diverse real-world datasets of human videos and zero-shot evaluations on completely unseen datasets demonstrate strong generalization and reasoning capabilities of *HandsOnVLM* for hand trajectory prediction given colloquial language instructions. Furthermore, the model outperforms most baselines on the Reasoning-based Hand Prediction (RBHP) task, showcasing its capability to reason and leverage world knowledge of VLMs.

## 2 RELATED WORK

We discuss prior works on human motion reconstruction and forecasting, developments in multi-modal large language models and action understanding from human videos.

---

## 2.1 HUMAN MOTION RECONSTRUCTION AND FORECASTING

Several prior works have attempted to recover hand meshes and full body meshes from human videos Rong et al. (2020); Pavlakos et al. (2024). Going beyond reconstruction, other works have also investigated forecasting motions of humans in the future. Early works used RNNs Bütepage et al. (2017; 2018); Honda et al. (2020) for anticipating future human poses, and recent approaches include Transformer architectures for more diverse and plausible future predictions Ding et al. (2023). More directly related to our work, some approaches predict egocentric hand-trajectories in the form of 2D waypoints (Liu et al., 2020), and others also predict object affordances jointly with hand trajectories (Liu et al., 2022). Some predict hand trajectories in a 3D space conditioned on a few RGB observations from an egocentric view Bao et al. (2023). Architectures for such egocentric predictions have ranged from transformers (Liu et al., 2022; Bao et al., 2023) to diffusion models Ma et al. (2024b;a) trained specifically for this prediction task. Our work extends this line of low-level egocentric trajectory prediction by enabling reasoning capabilities through augmentation and joint training with a pre-trained VLM.

## 2.2 MULTIMODAL LARGE LANGUAGE MODELS

Our work is enabled by developments in multimodal Large Language Models that augment vision and language reasoning in a unified model. Such models like LLaVA (Liu et al., 2024) and Video-ChatGPT (Maaz et al., 2023) have enabled large-scale video understanding and localization of temporal events (semantic actions) in videos (Huang et al., 2024). Adjacently, other works have sought to make the inputs to the VLMs more flexible and informal through automatic segmentations of language instructions (Lai et al., 2024; Yang et al., 2023) and visual grounding allowing flexibility to process both image and region inputs (Rasheed et al., 2024). Recent works have extended the capabilities of VLMs to diverse domains including robotic navigation (Zhang et al., 2024a), robotic manipulation (Kim et al., 2024; Brohan et al., 2023), spatial reasoning Cheng et al. (2024), and reasoning about 3D human poses from images and text Feng et al. (2024). While these approaches are orthogonal to our task of egocentric hand trajectory prediction, they serve as evidence of the potential of VLMs for downstream applications.

## 2.3 ACTION RECOGNITION AND PREDICTION FROM VIDEOS

Understanding actions in the form of what is happening in a video segment has a long history in computer vision (Sigurdsson et al., 2017; Liu et al., 2021; Kovashka & Grauman, 2010; Feichtenhofer et al., 2019). Several benchmarks and datasets containing human videos and action labels for tasks have also been proposed for related problems (Grauman et al., 2022; Caba Heilbron et al., 2015; Goyal et al., 2017). Our work leverages such datasets and goes beyond *recognition* of actions in videos to *prediction* of low-level actions in the future by first reasoning about future high-level actions through a VLM. As such our work can have potential applications in robotics for learning motion from web videos for manipulation by complementing prior works in this space (Bharadhwaj et al., 2024a; Bahl et al., 2023; Bharadhwaj et al., 2024b; Nair et al., 2022).

# 3 APPROACH

*HandsOnVLM* is a video-based VLM with the capability of predicting future hand trajectories given a video context and language instructions. There are three key components of *HandsOnVLM*'s architecture: (1) SlowFast tokens to capture temporal information at fine temporal resolution, (2) hand representation using an augmented vocabulary of  $\langle \text{HAND} \rangle$  token, and (3) iterative hand decoding to enable auto-regressive trajectory training and inference. In the training stage, we fine-tune a pre-trained VLM by combining next-token prediction loss and trajectory loss.

## 3.1 ARCHITECTURE

We show an overview of the *HandsOnVLM* model architecture in Fig 2. *HandsOnVLM* takes a sequence of  $T$  frames  $X_v$  and a language instruction  $X_q$  as input and predicts future hand trajectories  $\mathcal{H} = \{h_{T+i}\}_1^N$ , where  $N$  is the future horizon. At each future time step  $T + i$ , the future hand location  $h_{T+i}$  consists of the 2D location of the center of the left and right hands projected to the

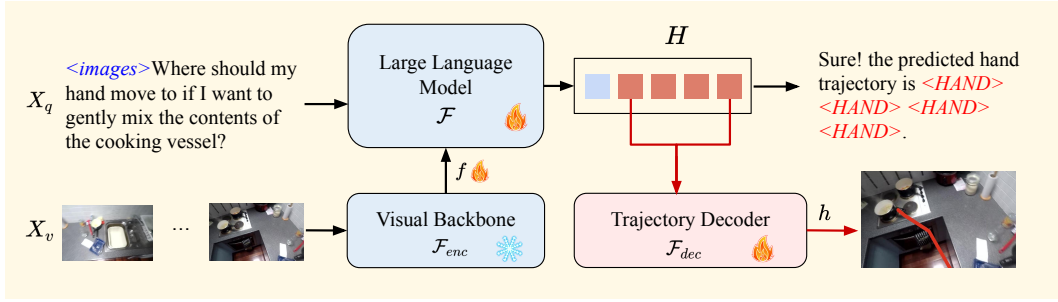


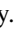



Figure 2: Overview of the *HandsOnVLM* architecture, where  and  denote trainable and frozen modules separately. *HandsOnVLM* casts hand trajectory prediction as an auto-regressive next-token prediction conditioned on fused video and language tokens. The architecture augments a pre-trained VLM with an additional hand token in the vocabulary. We use  and  to represent text and  $\langle \text{HAND} \rangle$  tokens respectively.

last observation frame  $X_v[-1]$ . The key components of the architecture include a visual backbone  $\mathcal{F}_{enc}$ , a vision-to-language projection layer  $f$ , a Large Language Model (LLM)  $\mathcal{F}$  and a trajectory decoder  $\mathcal{F}_{dec}$ .

**SlowFast Token Compression.** To obtain a capable video-conditioned VLM we need to be able to interpret temporal information at a fine resolution. Following Huang et al. (2024), given  $X_v$ , we embed them into  $T \times M$  visual tokens using a visual backbone, where  $M$  is the number of tokens in each frame. Then we apply slow-fast pooling to get  $T + M$  visual tokens. In the fast path, we average all the tokens within each frame to get  $T$  tokens overall. We also uniformly select  $s$  frames among all  $T$  frames and perform  $s \times s$  spatial average pooling to get  $M$  slow frames in total. These slow tokens will help preserve spatial information during the encoding process. Then we embed and align  $T + M$  visual tokens to the language space through a vision-to-language projector  $f(\cdot)$ .

**Hand as Embedding.** To represent hand in the language space, we extend the existing vocabulary with a new  $\langle \text{HAND} \rangle$  token. However, a typical embedding layer would encode each  $\langle \text{HAND} \rangle$  token identically, resulting in individual  $\langle \text{HAND} \rangle$  token being indistinguishable from one another. To overcome this limitation, we embed ground truth hand positions into the  $\langle \text{HAND} \rangle$  tokens during the tokenization process. We feed them into the Large Language Model backbone and get the embedding of the last layer  $H$ , where  $H = \mathcal{F}(X_q, f(\mathcal{F}_{enc}(X_v)))$ .

**Iterative Hand Decoding.** For  $i$ -th token in the sequence, let  $H_i$  be the last-layer embedding of this token from the Large Language Model. *HandsOnVLM* decode it to predict the  $(i + 1)$ -th token as LLMs do. When  $(i + 1)$ -th token is a  $\langle \text{HAND} \rangle$  token, we input  $H_i$  into a hand trajectory decoder  $\mathcal{F}_{dec}$  to predict the hand position of the  $(i + 1)$ -th token  $h_{i+1} = \mathcal{F}_{dec}(H_i)$ . During inference, this decoded position is then encoded into the corresponding  $\langle \text{HAND} \rangle$  token embedding for following prediction rounds. In this way, we ensure that each subsequent prediction is conditioned on all previously predicted hand positions, maintaining temporal consistency and spatial awareness throughout the inference process and mitigating compounding errors.

### 3.2 TRAINING OBJECTIVES

The model is trained end-to-end using a text generation loss  $\mathcal{L}_{\text{txt}}$  and a hand trajectory prediction loss  $\mathcal{L}_{\text{hand}}$ . The overall objective  $\mathcal{L}$  is the weighted sum of both losses, determined by  $\lambda_{\text{txt}}$  and  $\lambda_{\text{hand}}$ :

$$\mathcal{L} = \lambda_{\text{txt}}\mathcal{L}_{\text{txt}} + \lambda_{\text{hand}}\mathcal{L}_{\text{hand}} \quad (1)$$

Specifically,  $\mathcal{L}_{\text{txt}}$  is the auto-regressive cross-entropy loss for text generation, and  $\mathcal{L}_{\text{hand}}$  is the hand prediction loss, which encourages the model to generate high-quality hand trajectories as well. Following Liu et al. (2022), we employ a reconstruction loss over future timesteps and a KL-Divergence Regularization loss as  $\mathcal{L}_{\text{hand}}$ :

$$\mathcal{L}_{\text{hand}} = \sum_{t=1}^N \mathcal{L}_{\text{recon}}(h_{T+t}, \hat{h}_{T+t}) + \mathcal{L}_{kl}(\mu_h, \sigma_h). \quad (2)$$



---

We employ CVAE (Sohn et al., 2015) as the hand trajectory decoder in this work (although the method is not tied to it). Thus,  $\mathcal{L}_{\text{recon}}$  is the MSE loss over valid hand positions, and  $\mu_h, \sigma_h$  here are the mean and the standard deviation that regularizes the latent z-space to be close to the normal distribution.

## 4 REASONING AND PREDICTING HAND TRAJECTORIES

In this section, we introduce two tasks: the Vanilla Hand Prediction (VHP) task, which extends the classic hand motion prediction (Liu et al., 2022), and the proposed Reasoning-based Hand Prediction (RBHP) task. Finally, we describe a two-step annotation-generating pipeline to build the corresponding RBHP dataset.

### 4.1 VANILLA HAND PREDICTION TASK

In this task, explicit action narration is required to predict the next hand motion. Here explicit means the action narration directly specifies the action and the target object without ambiguity, such as “cut the paper” or “open the microwave”. We choose Epic-Kitchen (Damen et al., 2018; 2022), H2O (Kwon et al., 2021) and FPHA (Garcia-Hernando et al., 2018) as datasets for this task. To generate the hand labels for all the datasets, following Liu et al. (2022), we first run an off-the-shelf active hand-object detector (Shan et al., 2020a) to get the hand bounding box in each frame. To get the ground truth of each future hand trajectory, we first compute pairwise homographies by matching SURF (Bay, 2006) features of masked regions through RANSAC and project each future hand position into the last observation frame. Then, we apply cubic Hermite spline interpolation to smooth the projected trajectories and fill any missing points. Finally, we filter the resulting trajectories with multiple criteria, including confidence thresholds, highest-score detection selection, feature matching thresholds, trajectory completeness checks, and boundary constraints.

To reformat these datasets for visual question answering, we structure them in a question-answer format using the following template:

*“USER:<images>, can you give me the future hand trajectory for {explicit action narration}? ASSISTANT: Sure, it is<HAND><HAND><HAND><HAND>.”*,

where  $\langle \text{images} \rangle$  represents a placeholder of visual tokens of the input frames. Note that the action is optional because we can also generate general templates without specifying the action, and in this case the task reduces to that in prior works Liu et al. (2022); Bao et al. (2023); Ma et al. (2024b).

### 4.2 REASONING-BASED HAND PREDICTION TASK

In addition to the Vanilla Hand Prediction Task, we introduce the Reasoning-based Hand Prediction (RBHP) task. Instead of utilizing explicit instructions to directly predict the hand motion, here the system is required to reason about it with implicit instructions. We define implicit instructions as colloquial language instructions that provide sufficient information for inferring the intended human hand action through reasoning, without explicitly naming the target object or action.

To construct a dataset for this task, we implement a two-step annotation-generating pipeline (Fig. 3) powered by GPT-4 (Achiam et al., 2023). This pipeline extracts implicit instructions from the Epic-Kitchens-100 dataset (Damen et al., 2022). Prompt templates for these two steps are provided in the Appendix A.5.

**Action-aware Image Description.** To get the implicit instructions, the first step is to generate a detailed description of the scene including all the objects in the foreground. We prompt GPT-4 with the ground truth action to capture action-related information, such as the physical properties of the target object or the spatial relationship with other objects.

**Implicit Action Generation.** Using the action-aware description of the scene, we are able to generate the implicit instructions using GPT-4 in a text template as follows:

*“USER:<images>, can you give me the future hand trajectory for {action implicit description}? ASSISTANT: Sure, it is<HAND><HAND><HAND><HAND>.”*

270  
271  
272  
273  
274  
275  
276  
277  
278  
279  
280  
281  
282  
283  
284  
285  
286  
287  
288  
289  
290  
291  
292  
293  
294  
295  
296  
297  
298  
299  
300  
301  
302  
303  
304  
305  
306  
307  
308  
309  
310  
311  
312  
313  
314  
315  
316  
317  
318  
319  
320  
321  
322  
323

### Classic Hand Trajectory Dataset

Action: Get the dough



### GPT-4 Action-aware Image Description

In the image, there is a countertop with various kitchen items. A white mixing bowl containing dough is positioned on the left, while a black baking tray sits in the center. The person's hand, covered in dough, is reaching towards the tray, suggesting they are about to transfer the dough. To the right, there is a frying pan with some cooked meat, and a blender is visible in the background. The overall scene depicts a busy kitchen environment, focused on food preparation.

### Implicit Action Generation

<images> What is the recommended hand movement for accessing the mixture in the white container?

### Visual Question-Answering Conversion

To accessing the mixture in the white container, the recommended hand trajectory is: <HAND><HAND><HAND><HAND>.

Figure 3: Illustration of the annotation pipeline for the RBHP task. By using GPT-4 on human video datasets we extract implicit language instructions for visual question-answering. The red and blue lines respectively show trajectories for the right and left hands.

We choose Epic-Kitchen and Ego4D (Grauman et al., 2022) as datasets for this task. Through the annotation-generating pipeline, we generate 7.5k question-answering pairs from Epic-Kitchen, and 8k pairs from Ego4D for zero-shot evaluation.

## 5 EXPERIMENT

We perform experiments for both the proposed tasks in order to answer the following research questions:

- How plausible are the hand trajectories produced by *HandsOnVLM*?
- Does *HandsOnVLM* exhibit reasoning abilities for implicit language queries?
- Does *HandsOnVLM* generalize zero-shot to unseen scenes from new datasets?

### 5.1 EXPERIMENT DETAILS

**Architecture.** Following LITA’s architecture, We use CLIP-L-14 (Radford et al., 2021) as the visual encoder and Vicuna (Chiang et al., 2023) as the LLM module. We adapt the vision-language projector from LLaVA (Liu et al., 2024) and have a CVAE (Sohn et al., 2015) as trajectory decoder. We use 4 frames for slow tokens and use average pool window  $s = 2$ . With 1 fast token per frame, this leads to a total of  $100 + 256 = 356$  tokens per video.

**Datasets.** For VHP and RBHP datasets, we sample 10 frames and predict the hand position in next 4 frames at 4 FPS. More details of dataset preparation can be found in Appendix A.1. In addition to our proposed datasets, *HandsOnVLM*<sup>†</sup> are also trained on a few additional datasets for five different tasks, namely ActivityNet-Captions (Krishna et al., 2017) and YouCook2 (Zhou et al., 2018) for dense video captioning and event localization, NExT-QA (Xiao et al., 2021) for video question answering, LLaVA-150K (Liu et al., 2024) for image instruction tuning, ActivityNet-RTL (Huang et al., 2024) for reasoning temporal localization. We co-train with these additional tasks to help with visual understanding and reasoning, and this is enabled by the flexible modeling of *HandsOnVLM* that allows training on generic QA datasets.

**Implementation Details.** For *HandsOnVLM* and other VLM-based baselines, in each epoch we select 24K samples from the Epic-Kitchens-100 VHP dataset. For *HandsOnVLM*<sup>†</sup>, in each epoch we randomly select 6K samples in Epic-Kitchens-100 VHP dataset, 6K in Epic-Kitchens-100 RBHP dataset and another 12K that are uniformly distributed among all other 5 tasks. We use a batch size of

Approach	BBox Input	On Validation Split						Zero-shot					
		EK55			EK100			H2O			FPHA		
		ADE ↓	FDE ↓	WDE ↓	ADE ↓	FDE ↓	WDE ↓	ADE ↓	FDE ↓	WDE ↓	ADE ↓	FDE ↓	WDE ↓
KF	✓	0.392	0.386	0.199	0.317	0.318	0.168	-	-	-	-	-	-
OCT	✓	0.216	0.199	0.105	0.209	0.187	0.102	-	-	-	-	-	-
OCT-global		0.232	0.218	0.115	0.216	0.193	0.105	-	-	-	-	-	-
LLaVA-Pixel2Seq		0.156	0.139	0.076	0.254	0.224	0.124	0.150	0.121	0.032	0.214	0.189	0.043
LLaVA-Traj		<b>0.126</b>	0.142	0.073	0.201	0.191	0.103	<b>0.133</b>	0.130	0.031	0.191	0.167	0.041
<i>HandsOnVLM</i>		0.136	<b>0.106</b>	<b>0.062</b>	<b>0.194</b>	<b>0.157</b>	<b>0.090</b>	0.135	<b>0.108</b>	<b>0.028</b>	<b>0.175</b>	<b>0.151</b>	<b>0.034</b>

Table 1: Comparison of VHP task with different baselines. We reported the performance on the validation split of Epic-Kitchen dataset. For the RBHP baselines, we also evaluate them on two unseen datasets, H2O and FPFA.

128, a learning rate of  $2e-5$  and train for 40 epochs. The total wall-clock time for training is around 36 hours for the 7B models while using 4 H100 GPUs. The LLM and vision-language projector are initialized with the LLaVA-1.5 pre-trained weights. During training, we freeze the visual backbone and fully fine-tune other modules.

## 5.2 METRICS AND BASELINES

Following previous works (Liu et al., 2022; Ma et al., 2024b) we use Average Displacement Error (ADE), Final Displacement Error (FDE) and Weighted Displacement Error (WDE) as metrics to evaluate VHP and RBHP tasks.

**Vanilla Hand Prediction.** For the VHP task, we choose Kalman Filter(KF) and Object-centric Transformer(OCT) (Liu et al., 2022) as the baselines. Since OCT still requires the bounding box feature of the hand and object as input, to get a fairer comparison with other end-to-end methods, we implement a version without the requirement of the bounding box, which we call OCT-global.

**Reasoning-based Hand Prediction.** To evaluate *HandsOnVLM*’s performance on the RBHP task, we perform baseline comparisons with several VLM-based methods. We describe these baselines below:

- **LLaVA-Traj.** Note that the hand trajectories are a sequence of pixel positions, we can represent them in text directly. In this case, we can directly fine-tune the LLaVA without any modification.
- **LLaVA-Pixel2Seq.** An alternative approach to representing hand positions involves quantizing the image into discrete spatial bins (Chen et al., 2021), each corresponding to a unique token. We can extend the existing vocabulary with those discrete tokens.
- **Language-conditioned Image-to-video Models.** We also compare our model to baselines of the language-conditioned image-to-video generation followed by hand-tracking. We use commercial state-of-the-art language-conditioned image-to-video systems such as LumaLabs (LumaLabs, 2024), Kling 1.5 (KlingAI, 2024) and generate videos conditioned on the last observation frame and the language description. Following the hand label generation process in Sec. 4.1, we track and extract the hand trajectories of the generated video.

## 5.3 COMPARISONS WITH BASELINES

We evaluate *HandsOnVLM* on both the VHP task and the proposed RBHP task and report the results and comparisons with baselines in Table 1 and Table 2 respectively. All models except *HandsOnVLM*<sup>†</sup> are trained on VHP datasets. *HandsOnVLM*<sup>†</sup> is trained on all available datasets (Data Combo 5 in Table 3).

**VHP Task.** We evaluate all the baselines on the VHP datasets as described in section 5.1. Here, the FPFA and H2O datasets serve as unseen datasets to test zero-shot generalization capabilities. Among all the VHP datasets, *HandsOnVLM* outperforms both the task-specific methods as well as the VLM-based methods, which demonstrates its strong ability to produce plausible trajectories corresponding to how a real human hand would move given explicit instructions. We also find that *HandsOnVLM* can generalize to completely unseen scenes (for example scenes from H2O and

FPHA datasets), which demonstrates it can effectively leverage the world knowledge of the pre-trained VLM.

**RBHP Task.** For evaluations on the RBHP task shown in Table 2, *HandsOnVLM* achieves state-of-the-art performance in all three metrics. This suggests that *HandsOnVLM* is able to reason based on implicit cues of the scene and be applied to complicated scenarios involving everyday natural language conversations. However, we observe that LumaLabs (LumaLabs, 2024) achieves the smallest ADE in the Ego4D RBHP benchmark but relatively higher FDE and WDE. This may be because the commercial text-conditioned image-to-video generation models have realistic video generation capabilities but cannot understand reasoning-based language prompts which is necessary for generating plausible videos maintaining temporal consistency. Since the training dataset compositions of these video models are not disclosed, there may also be some data leakage issues of the evaluation datasets in this paper being a part of their training corpora.

#### 5.4 ABLATION STUDY

In this section, we conduct a broad study of the different components of our model. All experiments in this section are evaluated on the RBHP task.

##### Effects of Different Sources of Dataset.

In Table 3, we show the contribution of each type of dataset to the performance of *HandsOnVLM*. LITA dataset denotes the dif-

ferent datasets for 5 additional tasks (Huang et al., 2024) described in Section 5.1 ranging from dense video captioning to reasoning about temporal localization. While increasing the scale of the VHP dataset (first two rows) can bring some improvement, we find that fine-tuning with the reasoning dataset (last two rows) can significantly boost the performance, even when fine-tuning with tasks that are not directly related to hand trajectory prediction. This demonstrates that *HandsOnVLM* can leverage world knowledge learned by other tasks to reason about predicting plausible hand trajectories.

Data Combos	Epic-Kitchen		LITA data	RBHP data	ADE↓	FDE↓	WDE↓
	55	100					
1	✓				0.206	0.195	0.101
2	✓	✓			0.197	0.165	0.094
3	✓	✓	✓		0.199	0.163	0.094
4	✓	✓	✓	✓	<b>0.187</b>	<b>0.156</b>	<b>0.089</b>

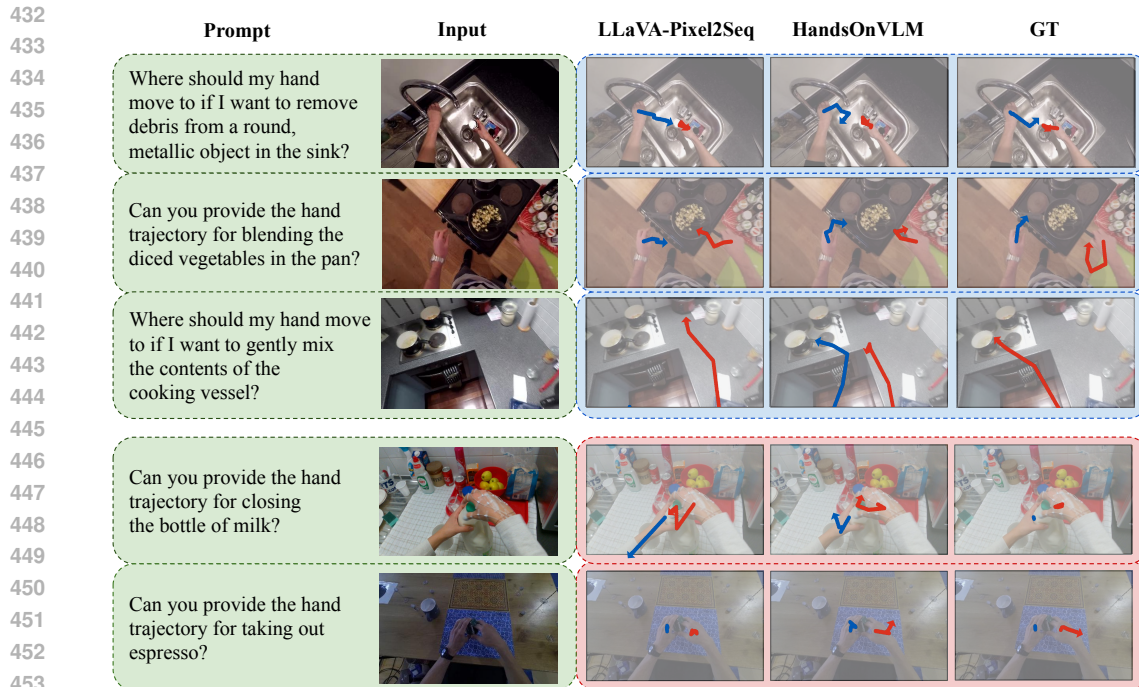
Table 3: Analysis of the impact of training data on the performance of *HandsOnVLM*. We can see that performance increases with additional data of VHP (first two rows), even with datasets of other tasks (third row), but the highest gains come from the proposed RBHP dataset (last rows).

##### Test-time Computation.

Recent works (Snell et al., 2024; OpenAI, 2024) have shown that using more test-time computation is a critical step for LLMs to improve their performance, especially on reasoning tasks. Motivated by these, we also investigate if such properties can enhance the performance of *HandsOnVLM* predictions. We report the performance using different numbers of generations during the stochastic decoding with self-consistency (Wang et al. (2023)) in Table 4. The main idea is to sample a

Num of Generations	ADE↓	FDE↓	WDE↓
1	0.187	0.156	0.089
4	0.184	0.152	0.087
8	<b>0.182</b>	0.151	<b>0.086</b>
16	<b>0.182</b>	<b>0.150</b>	<b>0.086</b>

Table 4: Analysis of test-time computations for *HandsOnVLM* in the form of stochastic decoding with self-consistency (Wang et al., 2023).



454 Figure 4: Qualitative results for different samples from the validation split of our RBHP dataset (top  
 455 in blue) and zero-shot evaluations on completely unseen datasets FPFA and H2O (bottom in pink).  
 456 The left-hand trajectory is visualized in blue and the right-hand trajectory is in red. The arrows  
 457 denote the direction of each trajectory. GT trajectories are provided for reference.

458  
 459 diverse set of reasoning paths instead of just one and then select the most consistent output through  
 460 marginalization. To obtain the self-consistency result in our context, we generate multiple answers  
 461 for each inquiry and then average the predicted hand trajectory. We find that increasing the test-time  
 462 computation in this form can robustly improve the performance of *HandsOnVLM* as seen by the  
 463 lower metrics from top to bottom in Table 4.

464 **Effect of different Observation Frames.** In Table 5, we investigate performance of our ap-  
 465 proach and the baselines when conditioned on just one observation frame instead of an observa-  
 466 tion video. Here we have four comparisons: OCT-last-im, OCT-global-last-im, *HandsOnVLM*-last-  
 467 im, *HandsOnVLM*<sup>†</sup>-last-im, which respectively correspond to versions of our baselines in Sec. 5.2  
 468 but are only conditioned on the last frame of the input video context. We find that the results in  
 469 this evaluation scenario are comparable to the setting where the context is a video, indicating that  
 470 *HandsOnVLM* can flexibly be conditioned on just one image when a video context is not available.

## 471 472 5.5 QUALITATIVE RESULTS

473  
 474 In Fig. 4 we show qualitative results  
 475 for *HandsOnVLM* and the strongest baseline  
 476 LLaVA-Pixel2Seq.  
 477 The section above the  
 478 horizontal line shows  
 479 visualization from  
 480 the validation split of  
 481 RHPB datasets, while  
 482 the section below the  
 483 line shows zero-shot  
 484 results on scenes from  
 485 completely unseen datasets.

Method	Num of Generations	ADE↓	FDE↓	WDE↓
VHP	OCT	0.209	0.187	0.102
	OCT-last-im	0.213	0.191	0.104
	OCT-global	0.216	0.193	0.105
	OCT-global-last-im	0.212	0.189	0.103
	<i>HandsOnVLM</i>	<b>0.194</b>	<b>0.157</b>	<b>0.090</b>
	<i>HandsOnVLM</i> -last-im	0.197	0.165	0.094
RBHP	<i>HandsOnVLM</i>	0.197	0.165	0.094
	<i>HandsOnVLM</i> -last-im	0.197	0.163	0.093
	<i>HandsOnVLM</i> <sup>†</sup>	<b>0.187</b>	0.156	0.089
	<i>HandsOnVLM</i> <sup>†</sup> -last-im	<b>0.187</b>	<b>0.155</b>	<b>0.088</b>

Table 5: Analysis of the number of observation frames during inference.



---

486 In the second row, we observe that *HandsOnVLM* generates a trajectory where the left hand stably  
487 holds the pan while the right hand performs the blending action. In contrast, LLaVA-Pixel2Seq fails  
488 to correctly depict holding the pan. The third row results demonstrates *HandsOnVLM*'s ability to  
489 reason about multi-modal solutions for the same task. While the ground truth shows the right hand  
490 moving the pot, *HandsOnVLM* chooses to use the left hand to execute the same action, illustrating  
491 its multi-modal reasoning ability capability.

## 492 493 6 CONCLUSION

494  
495 **Summary.** In this work, we propose *HandsOnVLM*, a novel video-based VLM to predict hand  
496 motion from ego-centric videos. We also proposed two tasks, Vanilla Hand Prediction(VHP) task  
497 and Reasoning-based Hand Prediction(RBHP) task to benchmark the hand motion prediction as  
498 well as the reasoning ability. We demonstrate its effectiveness through extensive quantitative and  
499 qualitative results. We believe this research represents a promising initial step towards integrating  
500 egocentric hand-object video understanding with the powerful capabilities of VLMs.

501 **Limitations.** While we enabled hand-trajectory prediction from colloquial language instructions,  
502 the quality of our predictions are bottle-necked by the limitations of ground-truth hand location  
503 extraction from videos, the models for which often fail when the hand is occluded or moving too  
504 fast. In addition, the 2D locations of hand we predict are not rich enough for directly being adapted  
505 for downstream applications like robotics and augmented reality.

506 **Future Work.** An interesting direction of future work would be to predict trajectories of full hand  
507 meshes in the future including orientation and articulation and also include depth in the predictions.  
508 Another exciting direction would be to adapt our model for long-horizon predictions for activities  
509 like “making coffee” which would consist of several steps and require reasoning over an extended  
510 period. Since video clips on the web have significant camera motion over time, a viable strategy for  
511 this could be chaining the model sequentially for different sub-tasks.

## 512 513 REPRODUCIBILITY STATEMENT

514  
515 We will provide the source code and the generated dataset including instructions on how to setup  
516 training and evaluation of the models. We have thoroughly reviewed our implementation and vali-  
517 dated its effectiveness through extensive experiments.

## 518 519 ETHICS STATEMENT

520  
521 Our paper focused on learning hand trajectories from human videos and language descriptions.  
522 There are many potential societal consequences of our work including deployments in AR/VR sys-  
523 tems and augmenting user experience for everyday activities by forecasting low-level actions in their  
524 egocentric frame of reference.

## 525 526 REFERENCES

527  
528 Josh Achiam, Steven Adler, Sandhini Agarwal, Lama Ahmad, Ilge Akkaya, Florencia Leoni Ale-  
529 man, Diogo Almeida, Janko Altenschmidt, Sam Altman, Shyamal Anadkat, et al. Gpt-4 technical  
530 report. *arXiv preprint arXiv:2303.08774*, 2023.

531  
532 Shikhar Bahl, Russell Mendonca, Lili Chen, Unnat Jain, and Deepak Pathak. Affordances from hu-  
533 man videos as a versatile representation for robotics. In *Proceedings of the IEEE/CVF Conference*  
534 *on Computer Vision and Pattern Recognition*, pp. 13778–13790, 2023.

535  
536 Wentao Bao, Lele Chen, Libing Zeng, Zhong Li, Yi Xu, Junsong Yuan, and Yu Kong. Uncertainty-  
537 aware state space transformer for egocentric 3d hand trajectory forecasting, 2023. URL <https://arxiv.org/abs/2307.08243>.

538  
539 Herbert Bay. Surf: Speeded up robust features. *Computer Vision—ECCV*, 2006.

- 
- 540 Homanga Bharadhwaj, Debidatta Dwivedi, Abhinav Gupta, Shubham Tulsiani, Carl Doersch, Ted  
541 Xiao, Dhruv Shah, Fei Xia, Dorsa Sadigh, and Sean Kirmani. Gen2act: Human video generation  
542 in novel scenarios enables generalizable robot manipulation. *arXiv preprint arXiv:2409.16283*,  
543 2024a.
- 544 Homanga Bharadhwaj, Roozbeh Mottaghi, Abhinav Gupta, and Shubham Tulsiani. Track2act: Pre-  
545 dicting point tracks from internet videos enables diverse zero-shot robot manipulation. *arXiv*  
546 *preprint arXiv:2405.01527*, 2024b.
- 547 Anthony Brohan, Noah Brown, Justice Carbajal, Yevgen Chebotar, Xi Chen, Krzysztof Choro-  
548 manski, Tianli Ding, Danny Driess, Avinava Dubey, Chelsea Finn, Pete Florence, Chuyuan Fu,  
549 Montse Gonzalez Arenas, Keerthana Gopalakrishnan, Kehang Han, Karol Hausman, Alex Her-  
550 zog, Jasmine Hsu, Brian Ichter, Alex Irpan, Nikhil Joshi, Ryan Julian, Dmitry Kalashnikov,  
551 Yuheng Kuang, Isabel Leal, Lisa Lee, Tsang-Wei Edward Lee, Sergey Levine, Yao Lu, Hen-  
552 ryk Michalewski, Igor Mordatch, Karl Pertsch, Kanishka Rao, Krista Reymann, Michael Ryoo,  
553 Grecia Salazar, Pannag Sanketi, Pierre Sermanet, Jaspiar Singh, Anikait Singh, Radu Soricut,  
554 Huang Tran, Vincent Vanhoucke, Quan Vuong, Ayzaan Wahid, Stefan Welker, Paul Wohlhart,  
555 Jialin Wu, Fei Xia, Ted Xiao, Peng Xu, Sichun Xu, Tianhe Yu, and Brianna Zitkovich. Rt-  
556 2: Vision-language-action models transfer web knowledge to robotic control. In *arXiv preprint*  
557 *arXiv:2307.15818*, 2023.
- 558 Judith Bütepage, Michael J. Black, Danica Kragic, and Hedvig Kjellström. Deep representation  
559 learning for human motion prediction and classification. In *2017 IEEE Conference on Computer*  
560 *Vision and Pattern Recognition (CVPR)*, pp. 1591–1599, 2017. doi: 10.1109/CVPR.2017.173.
- 561 Judith Bütepage, Hedvig Kjellström, and Danica Kragic. Anticipating many futures: Online human  
562 motion prediction and generation for human-robot interaction. In *2018 IEEE International Con-*  
563 *ference on Robotics and Automation (ICRA)*, pp. 4563–4570, 2018. doi: 10.1109/ICRA.2018.
- 564 8460651.
- 565 Fabian Caba Heilbron, Victor Escorcia, Bernard Ghanem, and Juan Carlos Niebles. Activitynet:  
566 A large-scale video benchmark for human activity understanding. In *Proceedings of the ieee*  
567 *conference on computer vision and pattern recognition*, pp. 961–970, 2015.
- 568 Ting Chen, Saurabh Saxena, Lala Li, David J Fleet, and Geoffrey Hinton. Pix2seq: A language  
569 modeling framework for object detection. *arXiv preprint arXiv:2109.10852*, 2021.
- 570 An-Chieh Cheng, Hongxu Yin, Yang Fu, Qiushan Guo, Ruihan Yang, Jan Kautz, Xiaolong Wang,  
571 and Sifei Liu. Spatialrgpt: Grounded spatial reasoning in vision language model. *arXiv preprint*  
572 *arXiv:2406.01584*, 2024.
- 573 Wei-Lin Chiang, Zhuohan Li, Zi Lin, Ying Sheng, Zhanghao Wu, Hao Zhang, Lianmin Zheng,  
574 Siyuan Zhuang, Yonghao Zhuang, Joseph E. Gonzalez, Ion Stoica, and Eric P. Xing. Vicuna: An  
575 open-source chatbot impressing gpt-4 with 90%\* chatgpt quality, March 2023. URL <https://lmsys.org/blog/2023-03-30-vicuna/>.
- 576 Dima Damen, Hazel Doughty, Giovanni Maria Farinella, Sanja Fidler, Antonino Furnari, Evangelos  
577 Kazakos, Davide Moltisanti, Jonathan Munro, Toby Perrett, Will Price, et al. Scaling egocentric  
578 vision: The epic-kitchens dataset. In *Proceedings of the European conference on computer vision*  
579 *(ECCV)*, pp. 720–736, 2018.
- 580 Dima Damen, Hazel Doughty, Giovanni Maria Farinella, Antonino Furnari, Evangelos Kazakos,  
581 Jian Ma, Davide Moltisanti, Jonathan Munro, Toby Perrett, Will Price, et al. Rescaling egocen-  
582 tric vision: Collection, pipeline and challenges for epic-kitchens-100. *International Journal of*  
583 *Computer Vision*, pp. 1–23, 2022.
- 584 Pengxiang Ding, Qiongjie Cui, Min Zhang, Mengyuan Liu, Haofan Wang, and Donglin Wang. Ex-  
585 pressive forecasting of 3d whole-body human motions. *arXiv preprint arXiv:2312.11972*, 2023.
- 586 Zicong Fan, Maria Pirelli, Maria Eleni Kadoglou, Xu Chen, Muhammed Kocabas, Michael J Black,  
587 and Otmar Hilliges. Hold: Category-agnostic 3d reconstruction of interacting hands and objects  
588 from video. In *Proceedings of the IEEE/CVF Conference on Computer Vision and Pattern Recog-*  
589 *nition*, pp. 494–504, 2024.

---

594 Christoph Feichtenhofer, Haoqi Fan, Jitendra Malik, and Kaiming He. Slowfast networks for video  
595 recognition. In *Proceedings of the IEEE/CVF international conference on computer vision*, pp.  
596 6202–6211, 2019.

597 Yao Feng, Jing Lin, Sai Kumar Dwivedi, Yu Sun, Priyanka Patel, and Michael J. Black. ChatPose:  
598 Chatting about 3d human pose. In *CVPR*, 2024.

600 Guillermo Garcia-Hernando, Shanxin Yuan, Seungryul Baek, and Tae-Kyun Kim. First-person hand  
601 action benchmark with rgb-d videos and 3d hand pose annotations. In *Proceedings of the IEEE*  
602 *conference on computer vision and pattern recognition*, pp. 409–419, 2018.

603 Mohit Goyal, Sahil Modi, Rishabh Goyal, and Saurabh Gupta. Human hands as probes for interac-  
604 tive object understanding. In *Proceedings of the IEEE/CVF Conference on Computer Vision and*  
605 *Pattern Recognition*, pp. 3293–3303, 2022.

607 Raghav Goyal, Samira Ebrahimi Kahou, Vincent Michalski, Joanna Materzynska, Susanne West-  
608 phal, Heuna Kim, Valentin Haenel, Ingo Fruend, Peter Yianilos, Moritz Mueller-Freitag, et al.  
609 The” something something” video database for learning and evaluating visual common sense. In  
610 *Proceedings of the IEEE international conference on computer vision*, pp. 5842–5850, 2017.

611 Kristen Grauman, Andrew Westbury, Eugene Byrne, Zachary Chavis, Antonino Furnari, Rohit Gird-  
612 har, Jackson Hamburger, Hao Jiang, Miao Liu, Xingyu Liu, et al. Ego4d: Around the world in  
613 3,000 hours of egocentric video. In *Proceedings of the IEEE/CVF Conference on Computer Vision*  
614 *and Pattern Recognition*, pp. 18995–19012, 2022.

615 Yutaro Honda, Rei Kawakami, and Takeshi Naemura. Rnn-based motion prediction in competitive  
616 fencing considering interaction between players. In *BMVC*, 2020.

618 De-An Huang, Shijia Liao, Subhashree Radhakrishnan, Hongxu Yin, Pavlo Molchanov, Zhiding  
619 Yu, and Jan Kautz. Lita: Language instructed temporal-localization assistant. *arXiv preprint*  
620 *arXiv:2403.19046*, 2024.

621 Kumara Kahatapitiya, Anurag Arnab, Arsha Nagrani, and Michael S Ryoo. Victr: Video-  
622 conditioned text representations for activity recognition. In *Proceedings of the IEEE/CVF Con-*  
623 *ference on Computer Vision and Pattern Recognition*, pp. 18547–18558, 2024.

625 Moo Jin Kim, Karl Pertsch, Siddharth Karamcheti, Ted Xiao, Ashwin Balakrishna, Suraj Nair,  
626 Rafael Rafailov, Ethan Foster, Grace Lam, Pannag Sanketi, et al. Openvla: An open-source  
627 vision-language-action model. *arXiv preprint arXiv:2406.09246*, 2024.

628 KlingAI. Kling ai. <https://klingai.com/>, 2024.

629

630 Takeshi Kojima, Shixiang Shane Gu, Machel Reid, Yutaka Matsuo, and Yusuke Iwasawa. Large  
631 language models are zero-shot reasoners. *Advances in neural information processing systems*,  
632 35:22199–22213, 2022.

633 Adriana Kovashka and Kristen Grauman. Learning a hierarchy of discriminative space-time neigh-  
634 borhood features for human action recognition. In *2010 IEEE computer society conference on*  
635 *computer vision and pattern recognition*, pp. 2046–2053. IEEE, 2010.

636

637 Ranjay Krishna, Kenji Hata, Frederic Ren, Li Fei-Fei, and Juan Carlos Niebles. Dense-captioning  
638 events in videos. In *Proceedings of the IEEE international conference on computer vision*, pp.  
639 706–715, 2017.

640 Taein Kwon, Bugra Tekin, Jan Stühmer, Federica Bogo, and Marc Pollefeys. H2o: Two hands  
641 manipulating objects for first person interaction recognition. In *Proceedings of the IEEE/CVF*  
642 *International Conference on Computer Vision (ICCV)*, pp. 10138–10148, October 2021.

643 Xin Lai, Zhuotao Tian, Yukang Chen, Yanwei Li, Yuhui Yuan, Shu Liu, and Jiaya Jia. Lisa: Rea-  
644 soning segmentation via large language model. In *Proceedings of the IEEE/CVF Conference on*  
645 *Computer Vision and Pattern Recognition*, pp. 9579–9589, 2024.

646

647 Haotian Liu, Chunyuan Li, Qingyang Wu, and Yong Jae Lee. Visual instruction tuning. *Advances*  
*in neural information processing systems*, 36, 2024.

---

648 Miao Liu, Siyu Tang, Yin Li, and James M Rehg. Forecasting human-object interaction: joint  
649 prediction of motor attention and actions in first person video. In *Computer Vision–ECCV 2020:*  
650 *16th European Conference, Glasgow, UK, August 23–28, 2020, Proceedings, Part I 16*, pp. 704–  
651 721. Springer, 2020.

652 Shaowei Liu, Subarna Tripathi, Somdeb Majumdar, and Xiaolong Wang. Joint hand motion and  
653 interaction hotspots prediction from egocentric videos. In *Proceedings of the IEEE/CVF Confer-*  
654 *ence on Computer Vision and Pattern Recognition (CVPR)*, 2022.

656 Xin Liu, Silvia L Pinteá, Fatemeh Karimi Nejadasl, Olaf Booij, and Jan C Van Gemert. No frame left  
657 behind: Full video action recognition. In *Proceedings of the IEEE/CVF conference on computer*  
658 *vision and pattern recognition*, pp. 14892–14901, 2021.

659 LumaLabs. Dream machine. <https://lumalabs.ai/dream-machine>, 2024.

661 Junyi Ma, Xieyuanli Chen, Wentao Bao, Jingyi Xu, and Hesheng Wang. Madiff: Motion-aware  
662 mamba diffusion models for hand trajectory prediction on egocentric videos. *arXiv preprint*  
663 *arXiv:2409.02638*, 2024a.

664 Junyi Ma, Jingyi Xu, Xieyuanli Chen, and Hesheng Wang. Diff-ip2d: Diffusion-based hand-object  
665 interaction prediction on egocentric videos. *arXiv preprint arXiv:2405.04370*, 2024b.

667 Muhammad Maaz, Hanoona Rasheed, Salman Khan, and Fahad Shahbaz Khan. Video-chatgpt:  
668 Towards detailed video understanding via large vision and language models. *arXiv preprint*  
669 *arXiv:2306.05424*, 2023.

670 Suraj Nair, Aravind Rajeswaran, Vikash Kumar, Chelsea Finn, and Abhinav Gupta. R3m: A univer-  
671 sal visual representation for robot manipulation. *arXiv preprint arXiv:2203.12601*, 2022.

672 OpenAI. Introducing OpenAI O1 preview, 2024. URL [https://openai.com/index/  
674 introducing-openai-o1-preview/](https://openai.com/index/introducing-openai-o1-preview/).

675 Georgios Pavlakos, Dandan Shan, Ilija Radosavovic, Angjoo Kanazawa, David Fouhey, and Jitendra  
676 Malik. Reconstructing hands in 3d with transformers. In *Proceedings of the IEEE/CVF Confer-*  
677 *ence on Computer Vision and Pattern Recognition*, pp. 9826–9836, 2024.

679 Alec Radford, Jong Wook Kim, Chris Hallacy, Aditya Ramesh, Gabriel Goh, Sandhini Agarwal,  
680 Girish Sastry, Amanda Aspell, Pamela Mishkin, Jack Clark, et al. Learning transferable visual  
681 models from natural language supervision. In *International conference on machine learning*, pp.  
682 8748–8763. PMLR, 2021.

683 Hanoona Rasheed, Muhammad Maaz, Sahal Shaji, Abdelrahman Shaker, Salman Khan, Hisham  
684 Cholakkal, Rao M. Anwer, Eric Xing, Ming-Hsuan Yang, and Fahad S. Khan. Glamm: Pixel  
685 grounding large multimodal model. *The IEEE/CVF Conference on Computer Vision and Pattern*  
686 *Recognition*, 2024.

687 Yu Rong, Takaaki Shiratori, and Hanbyul Joo. Frankmocap: Fast monocular 3d hand and body  
688 motion capture by regression and integration. *arXiv preprint arXiv:2008.08324*, 2020.

689 Dandan Shan, Jiaqi Geng, Michelle Shu, and David F Fouhey. Understanding human hands in  
690 contact at internet scale. In *Proceedings of the IEEE/CVF conference on computer vision and*  
691 *pattern recognition*, pp. 9869–9878, 2020a.

692 Dandan Shan, Jiaqi Geng, Michelle Shu, and David F Fouhey. Understanding human hands in  
693 contact at internet scale. In *Proceedings of the IEEE/CVF conference on computer vision and*  
694 *pattern recognition*, pp. 9869–9878, 2020b.

695 Gunnar A Sigurdsson, Olga Russakovsky, and Abhinav Gupta. What actions are needed for un-  
696 derstanding human actions in videos? In *Proceedings of the IEEE international conference on*  
697 *computer vision*, pp. 2137–2146, 2017.

700 Charlie Snell, Jaehoon Lee, Kelvin Xu, and Aviral Kumar. Scaling llm test-time compute optimally  
701 can be more effective than scaling model parameters. *arXiv preprint arXiv:2408.03314*, 2024.

---

702 Kihyuk Sohn, Honglak Lee, and Xinchun Yan. Learning structured output representation using deep  
703 conditional generative models. In C. Cortes, N. Lawrence, D. Lee, M. Sugiyama, and R. Garnett  
704 (eds.), *Advances in Neural Information Processing Systems*, volume 28. Curran Associates, Inc.,  
705 2015.

706 Xuezhi Wang, Jason Wei, Dale Schuurmans, Quoc V Le, Ed H. Chi, Sharan Narang, Aakanksha  
707 Chowdhery, and Denny Zhou. Self-consistency improves chain of thought reasoning in language  
708 models. In *The Eleventh International Conference on Learning Representations*, 2023.

709 Jason Wei, Xuezhi Wang, Dale Schuurmans, Maarten Bosma, Fei Xia, Ed Chi, Quoc V Le, Denny  
710 Zhou, et al. Chain-of-thought prompting elicits reasoning in large language models. *Advances in  
711 neural information processing systems*, 35:24824–24837, 2022.

712 Junbin Xiao, Xindi Shang, Angela Yao, and Tat-Seng Chua. Next-qa: Next phase of question-  
713 answering to explaining temporal actions. In *Proceedings of the IEEE/CVF conference on com-  
714 puter vision and pattern recognition*, pp. 9777–9786, 2021.

715 Senqiao Yang, Tianyuan Qu, Xin Lai, Zhuotao Tian, Bohao Peng, Shu Liu, and Jiaya Jia. An  
716 improved baseline for reasoning segmentation with large language model. *arXiv preprint  
717 arXiv:2312.17240*, 2023.

718 Jiazhao Zhang, Kunyu Wang, Rongtao Xu, Gengze Zhou, Yicong Hong, Xiaomeng Fang, Qi Wu,  
719 Zhizheng Zhang, and He Wang. Navid: Video-based vlm plans the next step for vision-and-  
720 language navigation. *arXiv preprint arXiv:2402.15852*, 2024a.

721 Zichen Zhang, Hongchen Luo, Wei Zhai, Yang Cao, and Yu Kang. Pear: Phrase-based hand-object  
722 interaction anticipation. *arXiv preprint arXiv:2407.21510*, 2024b.

723 Luowei Zhou, Chenliang Xu, and Jason Corso. Towards automatic learning of procedures from web  
724 instructional videos. In *Proceedings of the AAAI Conference on Artificial Intelligence*, volume 32,  
725 2018.

726  
727  
728  
729  
730  
731  
732  
733  
734  
735  
736  
737  
738  
739  
740  
741  
742  
743  
744  
745  
746  
747  
748  
749  
750  
751  
752  
753  
754  
755



756 A APPENDIX

757  
758 Here we provide additional details of the model implementation, dataset curation, and more qualita-  
759 tive results.

761 A.1 DATASET DETAILS

762  
763 **Statistics.** Table 6 shows the statistics of all datasets used in our tasks. Note that H2O, FPFA and  
764 Ego4D are only used for zero-shot evaluation so there are no training samples.

765

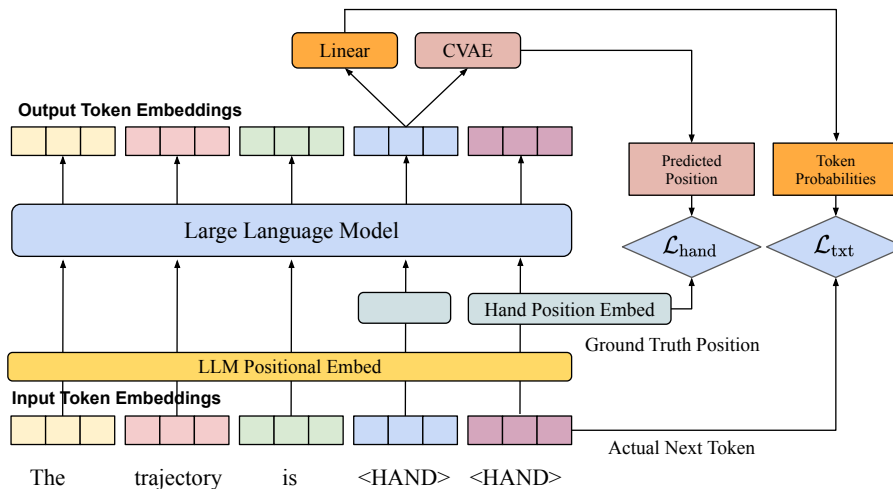
Task	Dataset	Training Samples	Validation Samples
VHP	Epic-Kitchen-55	8523	1894
	Epic-Kitchen-100	24148	3513
	H2O	-	503
	FPFA	-	501
RBHP	Epic-Kitchen-100	4018	3513
	Ego4D	-	8673

766  
767  
768  
769  
770  
771  
772

773 Table 6: Data Statistics of VHP and RBHP task.

774  
775  
776 A.2 PIPELINE DETAILS

777 Here we provide the illustrations of the training pipeline and the inference pipeline.



798 Figure 5: Illustration of training pipeline.

799  
800 A.3 OTHER ABLATION STUDIES

801  
802 **Scaling Model Improves the Prediction.** To evaluate the scaling ability of our model, we use  
803 LLaVA-V1.5-7B and LLaVA-V1.5-13B as the LLM backbone of our model. We refer them  
804 as *HandsOnVLM-7B* and *HandsOnVLM-13B*. We show the performance of both models in Fig.  
805 7.

806 **Zero-shot Chain-of-thought.** We also conduct an ablation study on the zero-shot chain-of-thought  
807 (Wei et al., 2022; Kojima et al., 2022) prompting, as shown in Fig. 8. We add “Let’s think step by  
808 step” in the front of the answer generated in the inference stage. Contrary to our expectations, this  
809 approach yielded poorer results. This unexpected outcome may be attributed to the limited diversity  
of our datasets.

810  
811  
812  
813  
814  
815  
816  
817  
818  
819  
820  
821  
822  
823  
824  
825  
826  
827  
828  
829  
830  
831  
832  
833  
834  
835  
836  
837  
838  
839  
840  
841  
842  
843  
844  
845  
846  
847  
848  
849  
850  
851  
852  
853  
854  
855  
856  
857  
858  
859  
860  
861  
862  
863

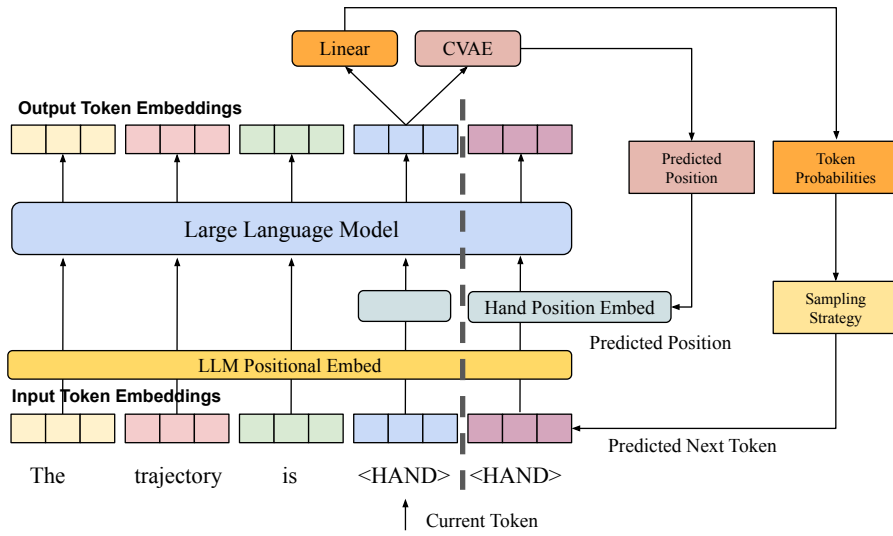


Figure 6: Illustration of inference pipeline.

Approach	ADE↓	FDE↓
<i>HandsOnVLM-7B</i>	0.197	0.165
<i>HandsOnVLM-13B</i>	<b>0.183</b>	<b>0.149</b>

Figure 7: Ablation study on the LLM backbone size. We evaluate them on the RBHP task.

Reasoning Method	ADE↓	FDE↓
Direct Answer	<b>0.197</b>	<b>0.165</b>
Chain-of-Thought	0.220	0.191

Figure 8: Comparison of direct answer and chain-of-thought reasoning methods.

#### A.4 MORE VISUALIZATIONS

**Failure Cases.** We show some failure cases in Fig. 9. We observe failures when (1) there are someone’s hands in the video, (2) the hands are occluded by objects, and (3) the target object in the instruction is not found in the frame.

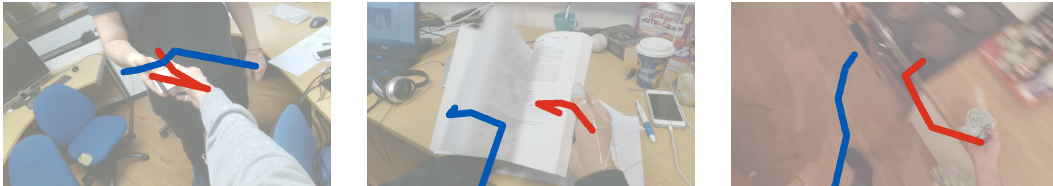


Figure 9: Failure cases of the model: (left) multiple hands in the video, (middle) occlusions, and (right) the target trash can is out of view.

**More Qualitative Results.** We provide more visualizations in Fig. 10.

#### A.5 PROMPT FOR VHP AND RBHP DATASET GENERATION

We provide the GPT4 prompts for the RBHP dataset generation pipeline mentioned in Section 4.2 in Table 7 and Table 8.

864  
865  
866  
867  
868  
869  
870  
871  
872  
873  
874  
875  
876  
877  
878  
879  
880  
881  
882  
883  
884  
885  
886  
887  
888  
889  
890  
891  
892  
893  
894  
895  
896  
897  
898  
899  
900  
901  
902  
903  
904  
905  
906  
907  
908  
909  
910  
911  
912  
913  
914  
915  
916  
917

<b>GPT4 Prompt for Action-aware Image Description</b>
You are a system generating descriptions for ego-centric human images. Human is doing household activities.
Provided with an image and a action narration of what is happening next, such as “use the scissor”, you will describe the main item that you see in the image, giving details but staying concise.
You can describe unambiguously what the item is, its color or relative position if clearly identifiable. You should also give out a overall description of the scene, the environment where the action is taking place.

Table 7: GPT4 prompt for action-aware image description.

<b>GPT4 Prompt for Implicit Action Generation</b>
You are tasked with creating specific, indirect questions and instructions that human could use to identify and interact with objects based on their names or detailed descriptions provided by users.
You will be given an action phrase which the human is going to do next, such as “use the scissor”.
Based on the descriptions, you must formulate responses that precisely hint at the action phrase without naming it directly. The aim is to enable the agent to deduce the correct action through these indirect cues, enhancing its ability to understand and execute tasks involving the object.
Please format your generated response as a hand trajectory question, some templates are provided below for reference: “Where should my hand move to if I want to {implicit description}” “Can you provide the hand trajectory for {implicit description}?” “What is the recommended hand movement for {implicit description}?”

Table 8: GPT4 prompt for implicit action generation.

<b>Question Templates to Build VHP Datasets.</b>
“Can you provide the hand trajectory?”
“What is the recommended hand movement?”
“What is the future hand trajectory in this video?”
“What is the predicted hand trajectory given current observations?”
“Where should my hand move to if I want to {explicit action}?”
“Can you provide the hand trajectory for {explicit action}?”
“What is the recommended hand movement for {explicit action}?”

Table 9: Question Templates to build VHP datasets.

<b>Answer Templates to build VHP and RBHP datasets.</b>
“Sure! Here is the hand trajectory {hand token sequence}.”
“Based on the video, the hand trajectory is as follows: {hand token sequence}.”
“The predicted hand trajectory is as follows: {hand token sequence}.”
“Certainly! The hand trajectory for {action instruction} is as follows: {hand token sequence}.”
“To {action instruction}, the recommended hand trajectory is: {hand token sequence}.”

Table 10: Answer Templates to build VHP and RBHP datasets.

918  
 919  
 920  
 921  
 922  
 923  
 924  
 925  
 926  
 927  
 928  
 929  
 930  
 931  
 932  
 933  
 934  
 935  
 936  
 937  
 938  
 939  
 940  
 941  
 942  
 943  
 944  
 945  
 946  
 947  
 948  
 949  
 950  
 951  
 952  
 953  
 954  
 955  
 956  
 957  
 958  
 959  
 960  
 961  
 962  
 963  
 964  
 965  
 966  
 967  
 968  
 969  
 970  
 971

Prompt	Input	LLaVA-Pixel2Seq	HandsOnVLM	GT
What is the recommended hand movement for transferring a bottle and its lid into their respective containers?				
Where should my hand move to if I want to transfer a delicious pizza from its parchment paper to a decorative dish?				
Where should my hand move to if I want to place a long, cylindrical baking tool into the wooden drawer?				
Where should my hand move to if I want to transfer the diced pieces of eggplant from the cutting board to the cooking vessel?				
Where should my hand move to if I want to transfer a delicious pizza from its parchment paper to a decorative dish?				
Where should my hand move to if I want to add a savory filling to the round pieces of dough?				
What is the recommended hand movement for taking out espresso?				
What is the recommended hand movement for opening milk box?				
Where should my hand move to if I want to clean glasses?				
What is the recommended hand movement for opening letter?				

Figure 10: More Qualitative results for different samples from the validation split of our RBHP dataset (top in blue) and zero-shot evaluations on completely unseen datasets FPFA and H2O (bottom in pink). GT trajectories are provided for reference.